

Single Stop Production at Hadron Colliders

T. Plehn*

Department of Physics, University of Wisconsin, Madison, WI 53706, USA

Abstract

We analyze the production of a single top squark at hadron colliders: $p\bar{p}/pp \rightarrow \tilde{t}_1 + X$. The total cross sections and the transverse momentum distributions are presented in next-to-leading order QCD. The higher-order corrections render the predictions theoretically stable with respect to variations of the factorization and renormalization scales. The transverse momentum distribution is resummed to estimate effects of the small transverse momentum regime on possible analyses. Since the corrections increase the cross sections and reduce the theoretical uncertainty, the discovery range for these particles is extended in the refined analysis.

Hadron colliders like the Tevatron and the LHC will soon be able to either discover or strongly constrain physics at scales well above the Standard Model masses. From an aesthetic point of view, the most attractive realization of supersymmetry could be the minimal supersymmetric model (MSSM). However, R parity conservation is an *ad hoc* assumption, invoked to bypass problems with flavor-changing neutral currents, proton decay, atomic parity violation and other experimental constraints. From a more general point of view, these observables put tight limits on some, but not on all, R parity violating couplings. For collider searches, exact R parity predicts that supersymmetric particles can only be pair-produced. Limited by the beam energy, the Tevatron tends to run out of supersymmetry discovery reach if the strongly interacting squarks and gluinos become too heavy to be produced in pairs. But many models based on unification scenarios at some high scale prefer exactly this kind of mass spectra. If, in contrast, R parity is not an exact symmetry, the signals from single superpartner production can be nicely extracted in the low background environment at the Tevatron [1–3] or even at the LHC [4].

In the case of a light scalar top squark, the baryon number violating coupling λ''_{ijk} induces the production process $\bar{d}_j \bar{d}_k \rightarrow \tilde{t}$ [2]. It stems from the superpotential contribution [5]

$$\mathcal{W} = \lambda''_{ijk} U_i^c D_j^c D_k^c, \quad (1)$$

where D^c and U^c denote charge conjugate right handed quark superfields. The couplings including at least one third generation flavor index $\{i, j, k\}$ are currently only constrained in the combination $|\lambda''_{313} \lambda''_{323}|$ [6,7]. The relevant Lagrangean reads¹

$$\mathcal{L}_{\lambda''} = -2\varepsilon^{\alpha\beta\gamma} \lambda''_{3jk} \left[\tilde{t}_{R\alpha} \overline{d_{j\beta}^c} P_R d_{k\gamma} + \text{h.c.} \right] + \dots \quad (j < k) \quad (2)$$

*Supported in part by DOE grant DE-FG02-95ER-40896 and in part by the University of Wisconsin Research Committee with funds granted by the Wisconsin Alumni Research Foundation.

¹Our conventions follow the leading order signal and background analysis [2].

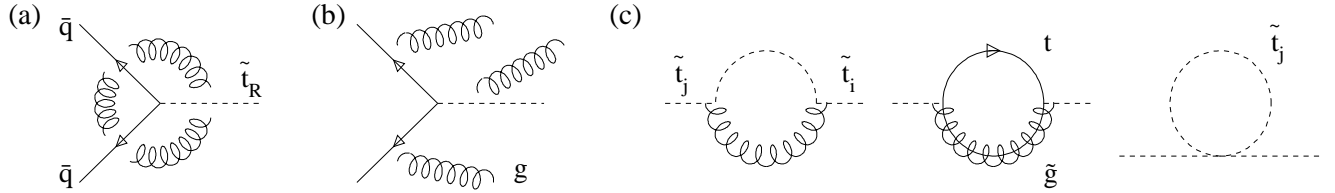


Figure 1. *Basic diagrams for the single stop production at hadron colliders in antiquark-antiquark collisions: (a) generic diagrams of virtual QCD corrections; (b) generic diagrams for real gluon emission; (c) SUSY-QCD corrections to the stop propagator, including the non-Standard Model contributions to the running mixing angle.*

If we assume that the R parity violating coupling is a small parameter $\lambda'' \lesssim 0.1$, and the stop is not too light, the produced single top squark has a sizeable branching fraction into the 'classical' supersymmetric channel $\tilde{t} \rightarrow b\tilde{\chi}^+$, where the light chargino decays to $l\nu\tilde{\chi}_1^0$ [2]. These decays have been calculated in next-to-leading order [8]; as expected for a decay mediated by the weak coupling constant, the corrections is moderate ($K \lesssim 1.2$), and the scale dependence is well under control. Furthermore, the higher order corrections leave the dependence on the stop mixing angle essentially unchanged.

Next-to-Leading Order Cross Section

In leading order the partonic cross section for the production of a single light top squark \tilde{t}_1 with the mass m is given by

$$\hat{\sigma}_{\text{LO}} = K_{qq} \frac{4\pi N_c(N_c - 1)}{m^2} \sin^2 \theta_t |\lambda''|^2 \delta\left(1 - \frac{m^2}{s}\right) \equiv K_{qq} \frac{\sigma_0}{m^2} \delta\left(1 - \frac{m^2}{s}\right); \quad K_{qq} = \frac{1}{4N_c^2}, \quad (3)$$

where the stop mixing angle θ_t measures the fraction of the right handed squark field in the light mixed state. During the following analysis we will omit this over-all factor, *i.e.* we assume $\tilde{t}_1 = \tilde{t}_R$. All cross sections can be scaled naively; we present the details of this argument below.

The $\mathcal{O}(\lambda''^2 \alpha_s)$ cross section includes virtual gluon contributions, as well as real gluon emission and the crossed channel with an incoming gluon (Fig. 1). The infrared and ultraviolet divergences are extracted using dimensional regularization. After adding virtual and real gluon contributions, and after renormalization, only collinear divergences remain. They are absorbed into the definition of the parton densities through mass factorization. Numerically we use the kinematical delta distribution in the Born cross section, eq(3), to perform the convolution of splitting functions and the leading-order cross section.

Diagrams involving heavy supersymmetric particles, like stops and gluinos, contribute to the virtual next-to-leading order matrix elements. From stop pair production [10], we know that the contribution of these loops is numerically well below the remaining theoretical and experimental uncertainties. Therefore we disregard them in the following analysis to remain maximally independent of the underlying model. In the case of single stop production there are no vertex diagrams involving gluinos/heavy stops.² The supersymmetric partners contribute through wave function renormalization of external quarks and stop legs. A second class of corrections arises from the Feynman diagrams shown in Fig. 1(c): the external light stop can mix to a heavy stop, which then couples to the incoming quarks. This is not part of the wave function renormalization, but it can be absorbed into a running stop mixing angle $\theta_t(\mu)$, evaluated at the external

²The coupling $d\tilde{d}\tilde{t}$ is in fact related to *e.g.* $\tilde{d}\tilde{d}\tilde{t}$ by supersymmetry, but since the latter is a three scalar soft breaking parameter we can assume $\lambda''_{\tilde{d}\tilde{d}\tilde{t}} \ll \lambda''_{d\tilde{d}\tilde{t}}$.

particle's mass scale. The Green's function with an external light stop leg will only depend on the heavy stop mass through the running mixing angle, *i.e.* the single stop production cross section will be proportional to $\sin \theta_t$ in leading and in next-to-leading order. The numerical effect of the running mixing angle has been shown to be negligible [8].

The hadronic $p\bar{p}$ and pp cross sections are obtained by folding the partonic cross section with parton luminosities. In leading order only $\bar{q}q$ initial states contribute to the production process. Especially for the production close to threshold, the gluon luminosity at the Tevatron is expected to be small. At the LHC, however, the $\bar{q}g \rightarrow \tilde{t} + \text{jet}$ cross section can be large. To estimate the gluonic contribution, we compute the total cross section for $\tilde{t} + \text{jet}$ production cross section (Tab. I). The transverse momentum is cut at a minimum value of 5 GeV. A resummed cross section, as it is derived later in this paper, cannot be used, since in the given order it does not distinguish clearly between the different incoming states. For a small stop mass of 200 GeV, 40% of the $\tilde{t} + \text{jet}$ events at the LHC involve an initial state gluon. This fraction drops to 25% for a stop mass of 500 GeV. Even at the Tevatron, light stops in association with a jet are produced through incoming gluons in 25% of the cases. This large fraction corresponds to the fact that for $\bar{q}q$ initial states the large valence quark luminosity does not contribute.

The next-to-leading order total cross sections are presented in Figure 2. The leading order results are in agreement with Ref. [2], after taking into account the large effect from switching the parton densities from CTEQ4M to CTEQ5M1. The next-to-leading order cross sections are parameterized by the factor $K = \sigma_{\text{NLO}}/\sigma_{\text{LO}}$. From the point of view of parton luminosities, both colliders are very similar; the initial state $\bar{d}s$ involves one valence and one sea quark, after summing over stop and anti-stop production. Therefore, the fraction of sea quarks and gluons in the proton dominates the K factor. For larger stop masses, the gluon luminosity at the Tevatron decreases rapidly; therefore the K factor drops to 1.15. At the LHC the change

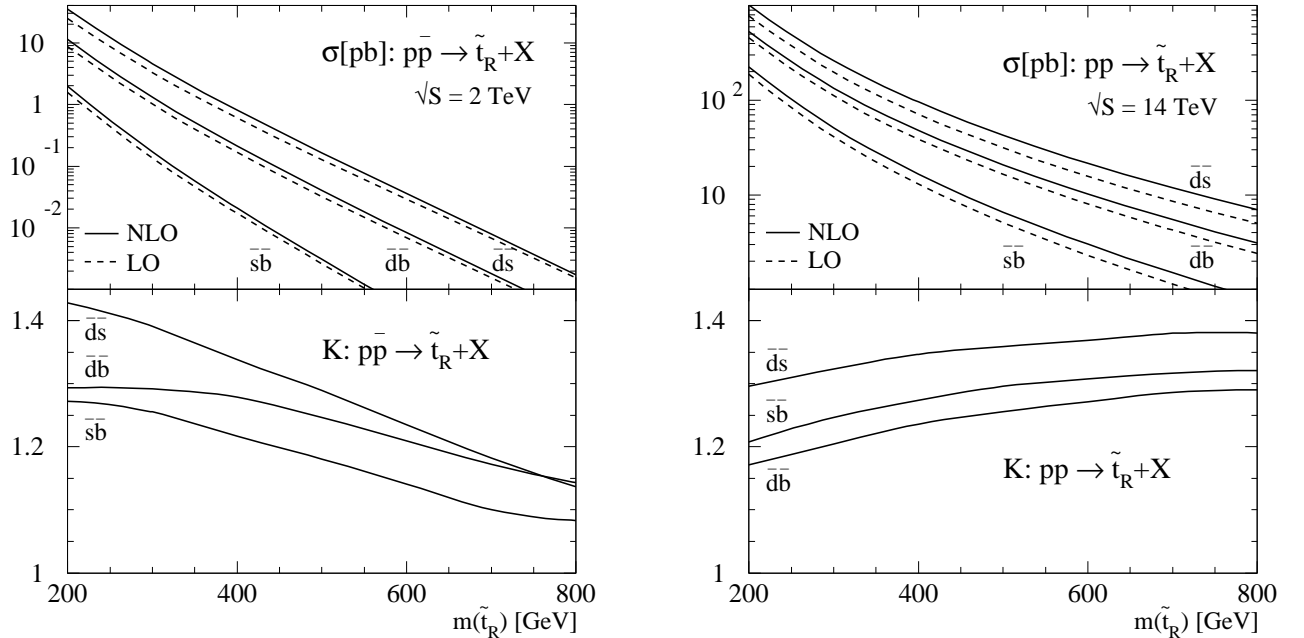


Figure 2. Total cross section and K factors for the single \tilde{t}_R production as a function of the mass. The couplings λ'' are all set to 0.1. The mixing angle dependence is omitted, $\sin \theta_t = 1$; the renormalization and factorization scales are fixed to the final state mass, and the parton densities used are CTEQ5L/M1 [11]. The curves are calculated for \tilde{t} plus \tilde{t}^* production for the three different couplings λ''_{ijk} . The dashed curves show the leading order, the solid curve the next-to-leading order results.

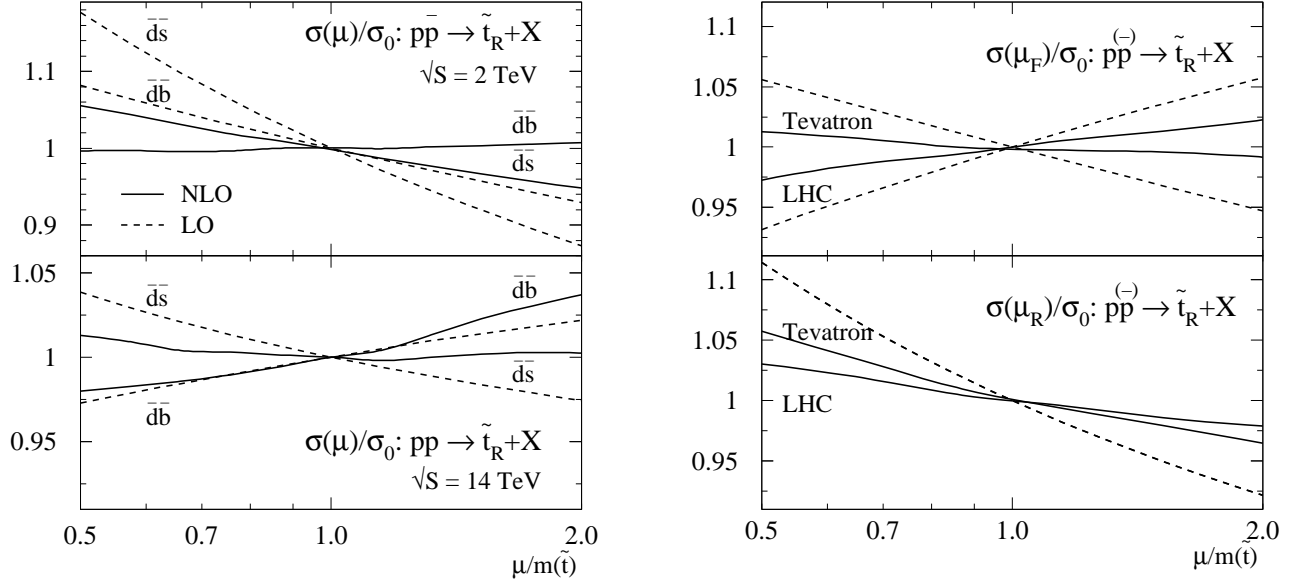


Figure 3. Renormalization and factorization scale dependence of the total cross section for a stop mass of 200 GeV, normalized to the central scale value $\mu = m$. Left: both scales are varied for two different initial states. The $\bar{s}\bar{b}$ case looks very similar to the $\bar{d}\bar{b}$ curve. Right: factorization and renormalization scale are varied independently. The respective other scale is fixed to the final state mass. The set of LO and NLO curves are given for the Tevatron and the LHC. Note that the leading order renormalization scale dependence at both colliders is identical. All unspecified parameters are chosen as in Fig.2.

is less dramatic. For the $\bar{d}\bar{s}$ initial state the K factor starts from a slightly smaller value than at the Tevatron and slowly increases from 1.3 to 1.4 with increasing mass.

One measure for the theoretical uncertainty coming from higher order corrections is the dependence of the cross sections on the renormalization and factorization scales. As a central value for both scales we use the final state mass ($\mu_F = \mu_R = m$). The dependence of the total cross section on the scales can be read off Fig. 3: identifying both scales and varying them between $m/2$ and $2m$ shows how the uncertainty is reduced by the next-to-leading order prediction. In case of a $\bar{d}\bar{s}$ initial state the uncertainty drops from 15% to 5% at the Tevatron and from 5% to even smaller values at the LHC. However, part of this unusually small scale dependence in leading and next-to-leading order is due to a cancellation between the factorization and the renormalization scale dependences. Especially at the LHC, the total scale dependence cancels out almost perfectly. Varying the scales independently yields an uncertainty of 10% in leading and 5% in next-to-leading order.

	m [GeV]	$\sigma_{\bar{t}}^{(\text{LO,CTEQ5L})}$	$\sigma_{\bar{t}}^{(\text{LO,CTEQ5M1})}$	$\sigma_{\bar{t}}^{(\text{NLO,CTEQ5M1})}$	$\sigma_{\bar{t}+g}^{(\text{CTEQ5M1})}$	$\sigma_{\bar{t}+q}^{(\text{CTEQ5M1})}$
Tevatron	200	24.70 pb	26.68 pb	35.28 pb	11.1 pb	3.81 pb
Tevatron	500	0.128 pb	0.113 pb	0.165 pb	0.057 pb	0.0099 pb
LHC	200	781 pb	865 pb	1013 pb	472 pb	321 pb
LHC	500	31.4 pb	35.7 pb	42.8 pb	29.2 pb	10.9 pb

TABLE I. The total cross sections for single stop production alone, together with a gluon jet, and through the crossed gluonic initial state together with a quark jet. For the latter the perturbative cross section has been used, cut at a minimum value of 5 GeV. All parameters are set as in Fig. 2.

The Coupling λ'' in Next-to-Leading Order

The R parity violating coupling $dd\tilde{t}_R$ is not an exclusive feature of the MSSM. The underlying model could as well be the Standard Model with an additional strongly interacting scalar; the coupling λ'' has no symmetry operation that connects it to any Standard Model coupling. The MSSM, however, adds new particles to the spectrum: the light-flavor squark, the left-handed scalar top quark, and the gluino can contribute to the next-to-leading order matrix element. For the process considered, the simple 'SM+ \tilde{t}_R ' model can be regarded as the low energy limit of the MSSM, after decoupling of the light-flavor squark, the heavy stop state and the gluino. In this case the diagrams involving any of these particles vanish; the projector on the right-handed stop state ($\sin \theta_t$) becomes unity or zero, dependent on if the lighter stop is the partner of the left or the right-handed top quark. Since the λ'' couples strongly interacting particles, it has to be renormalized [9]. Starting out from the known renormalization constants with and without heavy supersymmetric particles

$$Z_2^{(q)} = 1 - \frac{\alpha_s C_F}{4\pi} \frac{1 + 1_{\text{MSSM}}}{\tilde{\epsilon}}; \quad Z_2^{(\tilde{t})} = 1 + \frac{\alpha_s C_F}{2\pi} \frac{1 - 1_{\text{MSSM}}}{\tilde{\epsilon}}; \quad Z_1^{(dd\tilde{t})} = 1 - \frac{3\alpha_s C_F}{4\pi} \frac{1}{\tilde{\epsilon}}, \quad (4)$$

the relation between the four renormalization constants for the vertex leads to a renormalization and subsequently a running of the R parity violating coupling λ'' . Since the heavy particles decouple at typical hadron collider scales, the coefficient of $\lambda''(\mu_R^2)$ is determined by the low energy effective model:

$$Z_{\lambda''} = 1 - \frac{3\alpha_s C_F}{4\pi} \frac{1}{\tilde{\epsilon}}; \quad \lambda''(\mu_R^2) = \frac{\lambda''(Q^2)}{1 + \frac{3\alpha_s C_F}{4\pi} \log \frac{\mu_R^2}{Q^2}} \quad (5)$$

The pole in the standard $\overline{\text{MS}}$ conventions is given as $\epsilon/\tilde{\epsilon} = (4\pi)^\epsilon \Gamma(1 - \epsilon)/\Gamma(1 - 2\epsilon)$. This treatment is analogous to the decoupling of heavy particles from the running of the strong coupling constant $\alpha_s(\mu_R)$.

The Cross Section for Small Transverse Momenta

The perturbative calculation of the next-to-leading order cross section as presented in the previous section needs to be modified to investigate the p_T distribution of the top squark. If the transverse momentum becomes much smaller than the other scales in the process, *i.e.* the mass of the produced particle, the convergence of the perturbation series in α_s deteriorates. The series in α_s has to be replaced by a series in $\alpha_s \log^2 Q^2/p_T^2$ [12–14]. It is possible to resum all terms at least as singular as p_T^{-1} in the differential cross section $d\sigma/dp_T$: the formalism has been successfully applied to Drell-Yan, single vector boson and vector boson pair, heavy quark, and single Higgs boson production [15–17]. We start from the leading order asymptotic cross section in the limit of small transverse momentum:

$$\frac{1}{\sigma_0} \frac{d\sigma^{\text{asym}}}{dp_T dy} = K_{qq} \frac{\alpha_s}{\pi} \frac{1}{Sp_T} \left[\left(A \log \frac{m^2}{p_T^2} + B \right) f_{\bar{q}}(x_1^0) f_{\bar{q}}(x_2^0) + \sum_{i=\bar{q},g} (f_i \circ P_{\bar{q} \leftarrow i})(x_1^0) f_{\bar{q}}(x_2^0) \right] + (x_1^0 \leftrightarrow x_2^0) \quad (6)$$

Here $x_{1,2}^0 = e^{\pm y} m/\sqrt{S}$ are the momentum fractions in the limit of small transverse momentum. The leading order coefficients for the single stop production can be extracted from the soft and collinear divergences in the perturbative result. In contrast to the heavy quark production case [17], they do not consist of a Drell-Yan type contribution and additional final state radiation terms. Since the coupling λ'' violates baryon number there is no analogue without final state radiation, *i.e.* without strong interaction charge in the final state. The leading divergence in p_T^{-1} is given by $A = 2C_F$ and $B = -4C_F$.

The resummed differential cross section involves the integration over the impact parameter space of a Sudakov-like form factor:

$$\frac{1}{\sigma_0} \frac{d\sigma^{\text{resum}}}{dp_T dy} = K_{qq} \frac{2p_T}{S} \int_0^\infty db \frac{b}{2} J_0(bp_T) W(b)$$

$$W(b) = \exp \left[- \int_{b_0^2/b^2}^{m^2} \frac{dq^2}{q^2} \frac{\alpha_s(q^2)}{2\pi} \left(A \log \frac{m^2}{p_T^2} + B \right) \right] f_{\bar{q}}(x_1^0) f_{\bar{q}}(x_2^0) + (x_1^0 \leftrightarrow x_2^0) \quad (7)$$

The integral in the exponent can be calculated analytically³; the boundary is canonically chosen as $b_0 = 2e^{-\gamma_E}$. The Bessel function $J_0(x)$ oscillates, and the amplitude numerically decreases only slowly for large transverse momenta. In this regime we use the expansion of the impact parameter integral for large p_T as compared to the lower limit of b in the Bessel period considered [16]. The factorization scale for the resummation has been chosen as the mass of the final state particle, and the parton densities are evaluated at the point $\mu = b_0/b$. However, it has been shown that the resummed cross section is ill-defined for $b > \Lambda_{\text{QCD}}$; we follow one way of parameterizing nonperturbative physics by substituting the form factor $W(b)$ by [13]

$$W(b) \rightarrow W(b_*) \exp \left[-b^2 g_1 - b^2 g_2 \log \frac{b_{\text{max}} m}{2} \right]; \quad b_* = \frac{b}{\sqrt{1 + b^2/b_{\text{max}}^2}} \quad (8)$$

The parameters $g_{1,2}$ can be fitted to Drell-Yan data [15], yielding $g_1 = 0.15 \text{ GeV}^2$ and $g_2 = 0.4 \text{ GeV}^2$. The cutoff scale for the nonperturbative physics we choose as $b_{\text{max}} = (2 \text{ GeV})^{-1}$. The numerical dependence on these parameters has been shown to be negligible [15]. It is possible to match the large and small transverse momentum formulae using a matching function

$$\frac{d\sigma^{\text{general}}}{dp_T dy} = \frac{d\sigma^{\text{pert}}}{dp_T dy} + \frac{1}{1 + (p_T/p_T^{\text{match}})^4} \left[\frac{d\sigma^{\text{resum}}}{dp_T dy} - \frac{d\sigma^{\text{asym}}}{dp_T dy} \right] \quad (9)$$

where the matching scale $p_T^{\text{match}} \sim m/3$ is the typical choice. For large transverse momentum the asymptotic and the resummed cross sections give arbitrary unphysical results; numerically their contribution to the general cross section is faded out by the matching function. For small transverse momentum the perturbative and the asymptotic function approach each other rapidly. The matching function smoothes out the behavior of the general solution in the transition region. The uncertainty induced by the particular choice of a matching function is only $\mathcal{O}(\alpha_s^2)$ [15].

The results of the resummation are presented in Figure 4. As expected from similar processes [15] the resummed cross section peaks at $p_T \sim 5 \text{ GeV}$. The perturbative and the asymptotic cross sections numerically agree very well for small transverse momenta $p_T \lesssim 2 \text{ GeV}$. Qualitatively the perturbative and the resummed cross sections agree for intermediate $p_T \gtrsim 10 \text{ GeV}$. However, quantitatively the matched and the perturbative cross sections can differ by up to 40% for $p_T \lesssim 60 \text{ GeV}$ at the Tevatron and $p_T \lesssim 100 \text{ GeV}$ at the LHC. As can be seen in Fig. 4, the differential cross sections drop sharply with increasing transverse momentum; the choice of p_T^{match} should be taken into account as a theoretical source of uncertainty.

³This requires a truncation of the running of the strong coupling constant to leading order. We have fixed the leading order Λ_{QCD} to reproduce the correct value for $\alpha_s(M_Z)$; this choice introduces a numerical uncertainty, since the average renormalization scale in the process might be considerably larger, *e.g.* for a stop mass of 500 GeV. Moreover, the fitted value of Λ_{QCD} for the CTEQ5M1 parton densities assumes a next-to-leading order running. Changing the QCD scale in the given limits yields a numerical variation of $\lesssim 5\%$ for the resummed cross section.

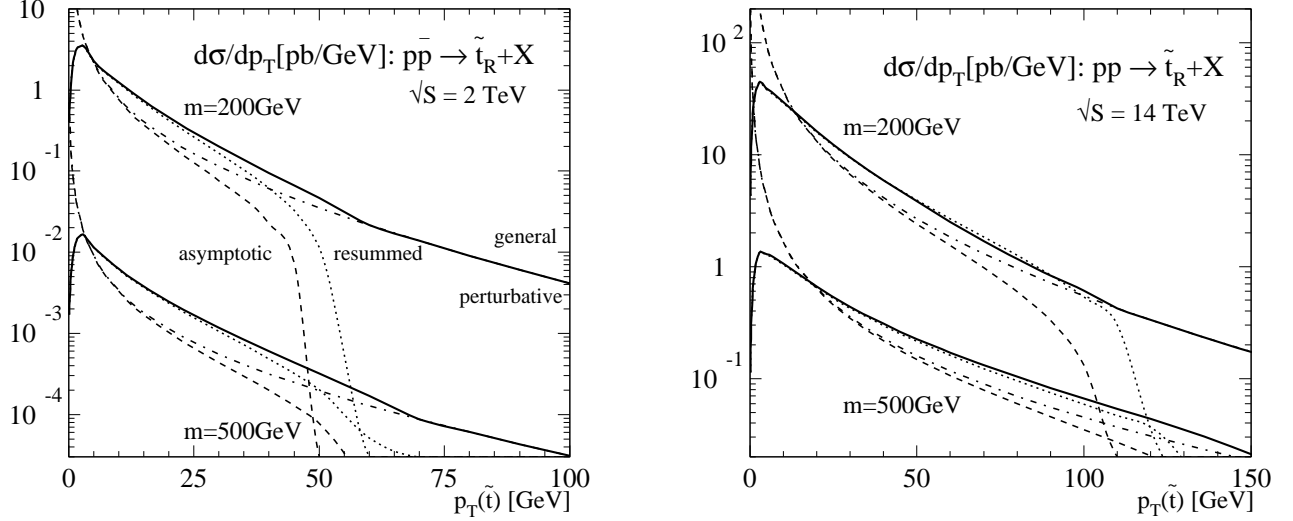


Figure 4. Differential transverse momentum distribution with respect to the top squark. The four different line styles denote the perturbative (dot dashed), asymptotic (dashed), resummed (dotted) and general (solid) cross sections, as described in the text. The two sets of curves correspond to stop masses of 200 and 500 GeV. All other parameters are chosen as in Fig.2.

Conclusions

It has been shown [2] that the search for single top squarks is a promising channel for the upgraded Tevatron. We have calculated the next-to-leading order signal and the \tilde{t} +jet production cross section. The total cross sections are enhanced by up to 30% at the Tevatron and 40% at the LHC. At both colliders, the crossed gluon-antiquark incoming states are important, since there is no pure valence quark production mechanism. However, the typical next-to-leading order features are similar to supersymmetric pair production processes. The factorization and renormalization scale dependence in next-to-leading order is reduced from typically 10% to 5% or less. The variation of both scales simultaneously results in strong cancellations. For the exclusive \tilde{t} +jet production we have resummed the leading large logarithms for small transverse momentum. The matched distributions exhibit some numerical dependence on the matching; especially for large stop masses at the LHC the resummation significantly enhances the differential cross sections up to a matching point $p_T^{\text{match}} \sim m/3$. Finally, we note that if we had a way to predict the helicity structure of the coupling λ'' , this process would currently be the only way to directly determine the stop mixing angle at a hadron collider [10].

Acknowledgments

We would like to thank T. Han, M. Spira and W. Beenakker for very helpful discussions and T. Falk for carefully reading the manuscript. Furthermore, we want to acknowledge the very pleasant discussions with B. Harris, Z. Sullivan and E.L. Berger, the authors of the original leading order analysis [2], which also inspired the calculation of the exclusive cross sections for small and large transverse momenta.

Bibliography

- [1] For a recent review see *e.g.* Physics at RunII: Workshop on Supersymmetry/Higgs hep-ph/9906224.
- [2] E.L. Berger, B.W. Harris and Z. Sullivan, Phys.Rev.Lett. 83 (1999) 4472.
- [3] K. Whisnant, J.-M. Yang, B.-L. Young, and X. Zhang, Phys.Rev. D56 (1997) 467; J.-M. Yang and B.-L. Young, Phys.Rev. D56 (1997) 5907.
- [4] H. Dreiner and G.G. Ross, Nucl.Phys. B365 (1991) 597; H. Dreiner, P. Richardson and M.H. Seymour, hep-ph/0001224; P. Chiappetta *et al.*, Phys.Rev. D61 (2000) 115008.
- [5] S. Weinberg, Phys.Rev. D26 (1982) 287; N. Sakai and T. Yanagida, Nucl.Phys. B197 (1982) 533.
- [6] See *e.g.* B. Allanach, A. Dedes and H. Dreiner, in [1].
- [7] P. Slavich, hep-ph/0003316.
- [8] H. Dreiner and G. Ross, Nucl.Phys. B365 (1991) 597; S. Kraml, H. Eberl, A. Bartl, W. Majerotto, and W. Porod, Phys.Lett. B386 (1996) 175; A. Djouadi, W. Hollik and C. Jünger, Phys.Rev. D55 (1997) 6975; W. Beenakker, R. Höpker, T. Plehn, and P.M. Zerwas, Z.Phys. C75 (1997) 349; T. Plehn, hep-ph/9809319.
- [9] T. Plehn, H. Spiesberger, M. Spira, and P.M. Zerwas, Z.Phys. C74 (1997) 611; Z. Kunszt and W. Stirling, Z.Phys. C75 (1997) 453.
- [10] M. Krämer, T. Plehn, M. Spira, and P.M. Zerwas, Phys.Rev.Lett. 79 (1997) 341; W. Beenakker, M. Krämer, T. Plehn, M. Spira, and P.M. Zerwas, Nucl.Phys. B515 (1998) 3; R. Demina, J. D. Lykken, K. T. Matchev, and A. Nomerotski, hep-ph/9910275.
- [11] H. Lai *et al.*, Eur.Phys.J. C12 (2000) 375.
- [12] J. Collins and D. Soper, Nucl.Phys. B193 (1981) 381; Nucl.Phys. B197 (1982) 446; Nucl.Phys. B213 (1983) 545E.
- [13] G. Parisi and R. Petronzio, Nucl.Phys. B154 (1979) 427.
- [14] For recent developments see *e.g.* R.K. Ellis and S. Veseli, Phys.Rev. D60 (1999) 011501.
- [15] I. Hinchliffe and S.F. Novaes, Phys.Rev. D38 (1988) 3475; R. Kauffman, Phys.Rev. D44 (1991) 1415; G. Altarelli, R.K. Ellis, M. Greco, and G. Martinelli, Nucl.Phys. B246 (1984) 12; C. Davies, B. Webber and W.J. Stirling, Nucl.Phys. B256 (1985) 413; T. Han, R. Meng and J. Ohnemus, Nucl.Phys. B384 (1992) 59; C. Balazs, E.L. Berger, S. Mrenna, and C.-P. Yuan, Phys.Rev. D57 (1998) 6934; C. Balazs and C.-P. Yuan, Phys.Lett. B478 (2000) 192.
- [16] P. Arnold and R. Kauffman, Nucl.Phys. B349 (1991) 381.
- [17] E. Laenen, W.L. van Neerven and J. Smith, Nucl.Phys. B369 (1992) 543; E.L. Berger and R. Meng, Phys.Rev. D49 (1994) 3248.